THE JOURNAL OF PHYSICAL CHEMISTRY A

Article

pubs.acs.org/JPCA

Antagonistic Interplay Between an Intermolecular CH···O and an Intramolecular OH···O Hydrogen Bond in a 1:1 Complex Between 1,2-Cyclohexanedione and Chloroform: A Combined Matrix Isolation Infrared and Quantum Chemistry Study

Amit Kumar Samanta,[†] Pujarini Banerjee,[‡] Biman Bandyopadhyay,[§] Prasenjit Pandey,[∥] and Tapas Chakraborty*[,‡]

[†]Center for Free-Electron Laser Science (CFEL), Deutsches Elektronen-Synchrotron DESY, 22607 Hamburg, Germany

[‡]Department of Physical Chemistry, Indian Association for the Cultivation of Science, Kolkata, India

[§]Department of Chemistry, Malaviya National Institute of Technology Jaipur, J. L. N. Marg, Jaipur, India

[∥]Department of Chemistry, Asutosh College, Kolkata, India

Supporting Information

ABSTRACT: Matrix isolation infrared spectra of a weak C−H···O hydrogen-bonded complex between the keto−enol form of 1,2-cyclohexanedione (HCHD) and chloroform have been measured. The spectra reveal that the intramolecular O−H···O H-bond of HCHD is weakened as a result of complex formation, manifesting in prominent blue shift (~23 cm^{-1}) of the ν_{O-H} band and red shifts (~7 cm^{-1}) of $\nu_{C=O}$ bands of the acceptor (HCHD). The ν_{C-H} band of donor $CHCl_3$ undergoes a large red shift of ~33 cm^{-1}. Very similar spectral effects are also observed for formation of the complex in CCl_4 solution at room temperature. Our analysis reveals that out of several possible iso-energetic conformational forms of the complex, the one involving antagonistic interplay between the two hydrogen bonds (intermolecular C−H···O and intramolecular O−H···O) is preferred. The combined experimental and calculated data presented here suggest that in condensed media, conformational preferences are guided by directional hyperconjugative charge transfer interactions at the C−H···O hydrogen bonding site of the complex.

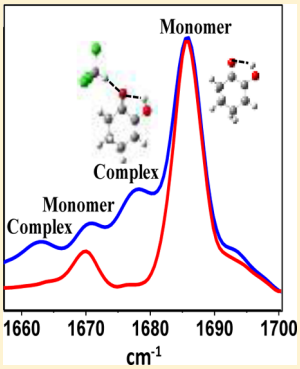

1. INTRODUCTION

Weak hydrogen bonds (HBs) have been the subject of intense studies in recent years.[1−44] Of particular interest are the CH···O hydrogen bonds,[15−44] which have been recognized as vital for structural stability and functioning of many biological macromolecules.[25−28] A lot of effort has been devoted to understanding the physical forces responsible for these weak molecular interactions, particularly with respect to the ways they differ from the conventional X−H···Y type hydrogen bonds,[2,3,15−22] where X and Y are two electronegative elements.

In earlier studies, the existence of CH···O hydrogen bonds was identified from crystallographic data, where shorter CH···O contacts in comparison to the sum of the van der Waals radii of respective CH groups and O atom were considered to be indicators of presence of such hydrogen bond.[23,24] In recent years, however, a variety of binary CH···O hydrogen bonded complexes have been identified in liquid and gas phases using vibrational spectroscopic methods, and infrared spectroscopy in particular has emerged as the method of choice for studying their spectroscopic properties.[30−44] A well-tested approach is to correlate the experimentally measured spectral shifts of suitable probe vibrational transitions at the hydrogen bonded sites with predictions of electronic structure calculations to understand the attributes of such bonding. Thus, quantum chemical methods have also established themselves as indispensable components in studies of weak hydrogen bonding.[30−44] An intriguing spectroscopic feature displayed by many of such complexes is the blue-shifting of the donor C−H stretching fundamental (ν_{C-H}).[15−22,34−41] Electronic structure studies have suggested that the factors responsible for blue shifts are not characteristically different from those responsible for red-shifting of the donor groups (X−H) in conventional (X−H···Y) hydrogen bonds. A subtle balance of all the factors determines whether the net spectral shift, in a particular case, would be blue or red.[15−22] In this context, a pertinent question is whether it is possible to predict intuitively the preferred mode of binding of a weak donor (C−H group) when more than one apparently similar acceptor site is present in the system. In the present work, we have addressed this issue through the study of a prototypical 1:1 complex between chloroform ($CHCl_3$) as HB donor and a cyclic α-diketone, 1,2-cyclohexanedione (CHD) as HB acceptor, and the competing binding sites are clearly indicated in Scheme 1.

Received: June 8, 2017
Revised: July 18, 2017
Published: July 24, 2017

DOI: 10.1021/acs.jpca.7b05615
J. Phys. Chem. A 2017, 121, 6012−6020

Scheme 1. Different Binding Sites on HCHD Molecule

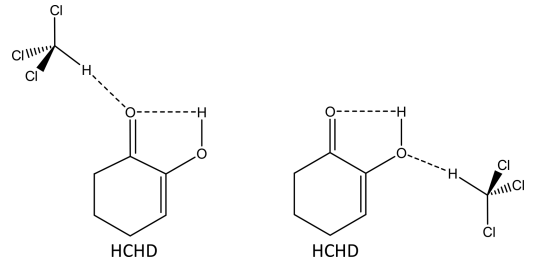

An α-diketo functional group belonging to a six-member cyclic ring is abundant in many natural products.[45] It has been shown in a number of recent studies that under experimental conditions where the molecules are practically isolated, e.g., in the vapor phase at low-pressure, in dilute solutions of nonpolar liquids or in cold inert-gas matrixes, CHD exists almost exclusively in monoenol tautomeric form (HCHD, Scheme 1) stabilized by an intramolecular OH···O hydrogen bond between the adjacent keto and enolic groups.[46] In the 1:1 complex with chloroform, the weak C−H donor group could potentially bind to two different sites on the acceptor, i.e the carbonyl oxygen or the enolic oxygen, resulting in different conformations of the complex (Scheme 1). In the former case, formation of the intermolecular CH···O HB is likely to weaken the intramolecular OH···O HB of the HCHD moiety since the carbonyl oxygen then becomes the common acceptor of two hydrogen bonds, i.e., the interplay between the two H-bonding interactions is antagonistic. Spectroscopically, such weakening of the OH···O HB is expected to lead to a blue-shift in the ν_{O-H} band of HCHD, because the O−H bond is strengthened. On the other hand, in the latter case, where the enolic group acts both as HB donor as well as acceptor, mutual cooperative effects could result in additional stability of the intramolecular OH···O HB, provided of course that weak intermolecular CH···O H-bonding contributes to cooperative stabilization in a sense similar to that in conventional hydrogen bonds. In this case, the donor O−H bond of HCHD would be weakened, and the ν_{O-H} frequency would thus be expected to undergo red-shifting. However, it is apparent that without taking into account the detailed interactions between the two molecules, it is not straightforward to predict the conformational preference qualitatively, or to predict whether one would be formed exclusively over the other.

In a recent matrix isolation study of a weak π-hydrogen bonded complex between formic acid and benzene, we had shown that while subtle variations in the intermolecular geometry do not largely affect overall binding energy predictions, experimental benchmarking is necessary to decipher the most stable geometry of a weakly bound complex.[6] In the present work, we provide convincing experimental data showing that only one conformational species is formed, although electronic structure calculations suggest possibilities of three conformers within a narrow energy range. The findings are interpreted in terms of short-range interactions at the site of C−H···O hydrogen bonding, which influence conformational preferences.

2. MATERIALS AND METHODS

2.1. Experimental Section. The apparatus used has been described in detail elsewhere.[46,47] CHD was procured from Aldrich and purified further by vacuum distillation. The FTIR spectra were recorded at a resolution of 0.5 cm^{-1} over an average of 32 scans each using a Bruker IFS66S Fourier transform infrared spectrometer, which is equipped with a deuterated triglycine sulfate (DTGS) detector and a KBr beam splitter. Spectral interferences from atmospheric water vapor and carbon dioxide were minimized by purging the spectrometer continuously with dry N_2. To prepare matrix-isolated samples, gas mixtures consisting of CHD vapor and chloroform in ultrahigh pure argon (~99.998%) in proportions of 1:1:500 were taken in a stainless steel chamber, and condensed for about an hour onto a thin KBr window cooled at ~8 K by a closed cycle helium refrigerator (Advanced Research Systems, Inc., model no. DE202). The deposition was carried out through a stainless steel deposition needle of diameter 500 μm, and a high precision needle valve (Swagelok) was used to regulate the deposition pressure of the premixed gas into the matrix chamber. On completion of deposition the spectra of the preannealed matrices were recorded after allowing the temperature to stabilize at 8 K. The matrix isolation condition was always verified during the course of deposition by analyzing the recorded FTIR spectra. The complex between chloroform and CHD was synthesized by annealing the initially deposited matrix to 27−30 K over about 30 min, and the spectra were recorded after recooling to 8 K. The temperature of the cold KBr substrate was monitored and controlled using a temperature controller (Lake Shore model 331). A homemade solution cell consisting of a pair of KBr windows and Teflon spacers of different thicknesses (250−500 μm) was used to study complex formation in CCl_4 solution. The solvent CCl_4 was procured from Spectrochem India Pvt. Ltd., and purified further by vacuum distillation.

2.2. Theoretical Calculations. The geometries of the tautomeric forms of CHD and its complexes with chloroform were optimized using the Gaussian 09 program package by density functional theory (DFT) methods, including dispersion corrected B97D and ωB97XD functionals.[48,49] The parametrized M06-2X method which is known to account reliably for dispersion interactions in weakly bound complexes was also used.[50] All calculations were performed at the 6-311++G(d,p) level of theory. Basis set superposition errors (BSSE) in calculated binding energies of the complexes were corrected using the counterpoise method of Boys and Bernardi.[51] The vibrational frequencies were computed by the same methods at a harmonic approximation, and have been reported here without the use of any scale factors, since the probes here are the complexation induced spectral shifts, which are less than 1% of the original frequencies. Natural bond orbital (NBO) analysis was performed on the optimized structures to obtain the populations in different bonding and antibonding orbitals, as well as hyperconjugation interaction energies between different orbitals on the donor−acceptor moieties.[52] The potential energy distributions (PED) of the normal vibrational modes of the monomers and complexes were calculated following the approach suggested by Pulay and Torok,[53] using Gamess (US) program package.[54] The localized molecular orbital method (LMO-EDA) was used for partitioning of the total interaction energies of the complex into its electrostatic, dispersion, polarization, and exchange constituents.[55]

3. RESULTS AND DISCUSSION

3.1. Matrix Isolation FTIR Spectra of the Complex. The spectral segments corresponding to $\nu_{C=O}$ and ν_{O-H} bands of

DOI: 10.1021/acs.jpca.7b05615
J. Phys. Chem. A 2017, 121, 6012−6020

HCHD in the FTIR spectra recorded under a matrix isolation condition are shown in Figures 1 and 2. Assignments for all the

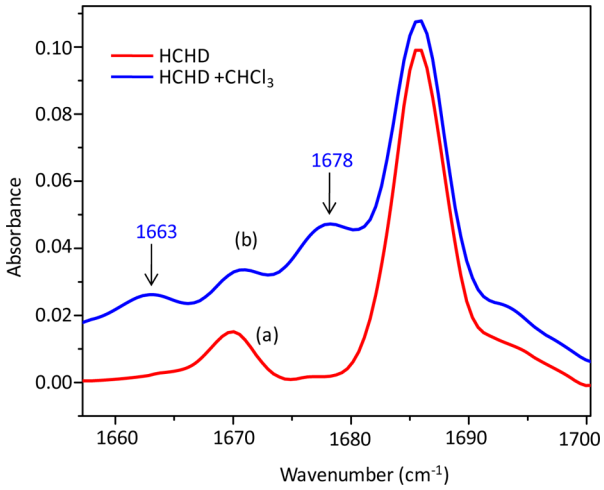

Figure 1. $\nu_{C=O}$ segment of the FTIR spectra of matrix isolated HCHD (red, trace a) and HCHD-$CHCl_3$complex (blue, trace b) obtained after annealing. The bands corresponding to complex formation are marked with arrows.

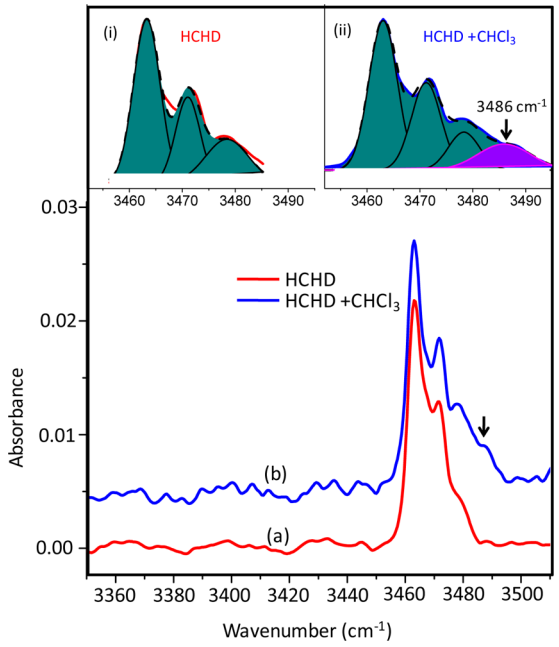

Figure 2. FTIR spectra in ν_{O-H} region of both matrix isolated HCHD (red, trace a) and HCHD-$CHCl_3$ complex (blue, trace b) obtained after annealing. Spectral fits both in the (i) absence and (ii) presence of $CHCl_3$ depicted in the insets help to identify the band corresponding to complex formation.

infrared spectral bands in the mid-IR spectrum of this molecule have been discussed earlier.[46] The molecule has been found to exist exclusively in monoenol tautomeric form (HCHD), and the $\nu_{C=O}$ band appears as a doublet due to symmetric and antisymmetric coupling of C═O and C═C stretching modes, both of which are infrared active and appear at 1685 and 1670 cm^{-1}, respectively (trace (a), Figure 1). The ν_{O-H} band of HCHD tautomer in the annealed matrix appears as a double-headed peak in the argon matrix, having maxima at ∼3463 and ∼3471 cm^{-1}, and there is an additional shoulder at ∼3478 cm^{-1} (trace (a), Figure 2). The multiple bands could be attributed to site effects within the argon matrix, or a weak polarization of the O−H group by the matrix leading to small shifts.

As a result of complex formation with $CHCl_3$, new bands corresponding to $\nu_{C=O}$ mode appear at 1678 and 1663 cm^{-1} [Trace (b), Figure 1], and both are red-shifted from the monomer $\nu_{C=O}$ components by 7 cm^{-1}. The shapes and relative intensities of these two new features remain unaffected for different mixing ratios of the two molecular components in the predeposition gas mixture, and are therefore attributed to a complex of 1:1 type. A noteworthy feature here is that the relative intensity of the two $\nu_{C=O}$ components of the complex is different from that of the bare molecule. Thus, the monomer band at 1685 cm^{-1} ($\nu_{C=O}^{A}$) is more intense compared to the lower frequency component at 1670 cm^{-1} ($\nu_{C=O}^{B}$). However, in case of the 1:1 complex, the two corresponding bands at 1678 and 1663 cm^{-1} appear with almost equal intensity. This attribute is more clearly manifested in the spectra measured under the liquid phase (see below).

Complex formation also gives rise to a new band at ∼3486 cm^{-1} in the ν_{O-H} spectral region, which appears at a blue shift of ∼23 cm^{-1} with respect to the most intense monomer ν_{O-H} band of HCHD at 3463 cm^{-1} [Trace (b), Figure 2]. A peak-fitting of the spectral profile in this region (shown in the inset) confirms the existence of this broad blue-shifted feature. The sign of the spectral shift indicates clearly that the intramolecular O−H···O HB of the molecule is weakened because of complex formation. As stated earlier, this could happen only if C−H of chloroform binds at the keto oxygen site of HCHD.

Spectral changes due to formation of the complex are also discernible in the ν_{C-H} region of $CHCl_3$ in the form of a broad and red-shifted feature (Figure 3). A fitting of the spectral profile reveals a new band with maximum at ∼3021 cm^{-1} (fwhm ∼20 cm^{-1}), which is red-shifted by 33 cm^{-1} from the monomeric ν_{C-H} band (3054 cm^{-1}). Calculation predicts many-fold enhancement in IR intensity of this band upon complex formation. The large increase of ν_{C-H} or ν_{C-D} intensity of the $CHCl_3$ or $CDCl_3$ donor as well as extensive broadening due to H-bond formation has been reported in a number of previous studies in inert gas matrices and cryosolutions, as well as in gas phase at room temperature.[8,34,56] However, the origin of the broadening has not been understood yet fully. We propose that the width for the present system is contributed by inhomogeneous broadening mechanisms originating from intensity borrowing via anharmonic coupling of ν_{C-H} ($CHCl_3$) with (i) the overtones and combinations in the fingerprint region, (ii) combinations with multiple low-frequency intermolecular vibrations of the complex, and (iii) C−H stretching fundamentals of HCHD. The predicted changes in this regard are presented in Supporting Information. It must also be noted that the bands at 3038 and 3045 cm^{-1} correspond to the self-association complex of $CHCl_3$, and we have noted that their intensities are enhanced upon annealing the matrix and on increasing the concentration of $CHCl_3$ in the gas mixture.

3.2. Complex Formation in CCl_4 Solution. To validate the observations in matrix, the complex between HCHD and $CHCl_3$ has also been studied in CCl_4 solution at room temperature. Figure 4 shows the $\nu_{C=O}$ and ν_{O-H} regions of the IR spectra measured for different ratios of the binary solution mixtures. With increase in HCHD to $CHCl_3$ mixing ratio, the maxima of both the $\nu_{C=O}$ components show distinct red shifts of ∼4 cm^{-1} (Figure 4 (upper panel)). The spectral fit, shown in

DOI: 10.1021/acs.jpca.7b05615
J. Phys. Chem. A 2017, 121, 6012−6020

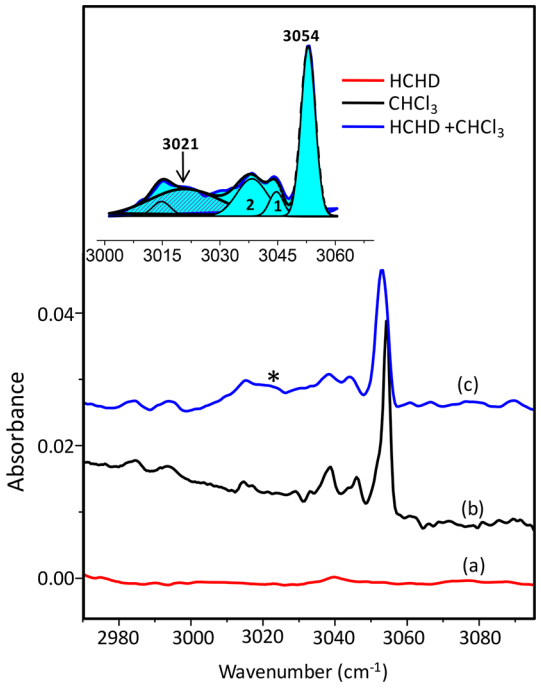

Figure 3. FTIR spectra depicting complex formation in ν_{C-H} region of $CHCl_3$. Traces (a) and (b) depict the spectra recorded after annealing the matrix containing only HCHD and $CHCl_3$ vapors in argon, respectively. Trace (c) depicts the spectrum of the annealed matrix of mixed vapors of HCHD and $CHCl_3$ in argon, where the asterisk marks the band due to complex formation. The spectral fitting in this region is shown in the inset. The fitted bands 1 and 2 correspond to self-association complexes of $CHCl_3$.

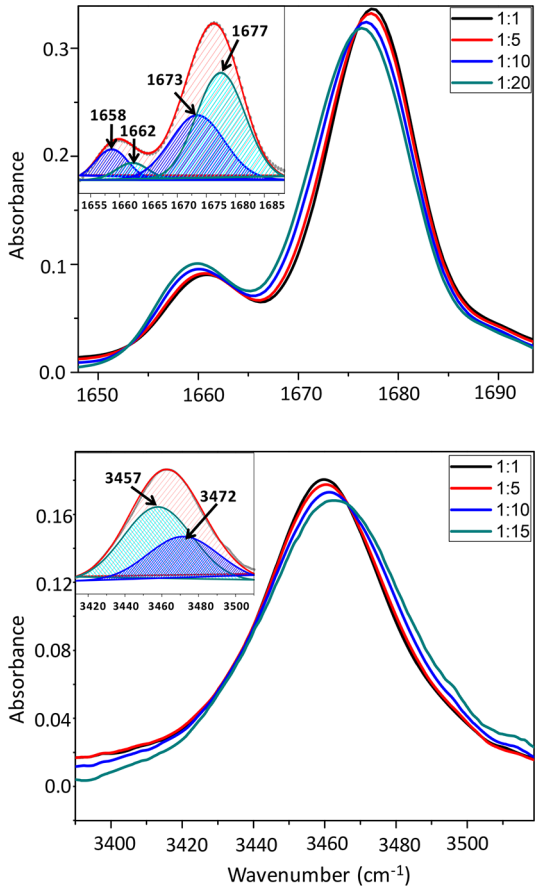

Figure 4. FTIR spectrum of HCHD-$CHCl_3$ complex in CCl_4 solution recorded for four different concentrations of $CHCl_3$ in the $\nu_{C=O}$ region (upper panel) and ν_{OH} region (lower panel). Curve fittings with Lorentzian functions showing bands corresponding to the complex are depicted in the insets.

the inset, indicates development of two similar new features for the complex in the lower wavenumber side, and the magnitude of these shifts are comparable to those observed in argon matrix. Second, the complex formation effect on relative intensities of the two $\nu_{C=O}$ components is more vividly manifested here, i.e., the lower frequency $\nu_{C=O}$ component of the complex appears much more intense with respect to the higher frequency component, compared to its relative intensity in the base molecule (HCHD). Thus, with increasing complex concentration in the solutions (curves 1 → 4), the overall intensity of the higher frequency component is reduced, but that of the lower frequency component is increased. An interpretation of this effect has been presented in section E in terms of changes in the potential energy distributions of the two normal modes upon complex formation.

The effect of complex formation on the ν_{O-H} transition is shown in the lower panel of Figure 4. With the increase in chloroform concentration, the band undergoes broadening, but the maximum is visibly shifted to higher frequency. Spectral fitting (inset) indicates that the ν_{O-H} band of the complex appears at ~15 cm^{-1} higher frequency compared to that of the monomer. Thus, the changes brought about by complex formation in this medium are consistent with those observed under matrix isolation conditions.

C. Complex Formation Effects Predicted by Theory. The optimized structures of two tautomeric forms of the bare molecule, CHD and HCHD, are shown in Figure 5a. The tautomer HCHD is predicted to be ~3 kcal/mol more stable, and it was shown previously that all the bands in the infrared spectrum of the matrix isolated sample could be assigned exclusively to this tautomer.[46] Therefore, in the present discussion, we consider only the HCHD tautomer of the molecule. Calculations predict three distinct conformers for the 1:1 complex of HCHD with $CHCl_3$, and their optimized structures and corresponding stabilization energies (ΔE_b) are shown in part (b) of Figure 5. In conformer I of the complex, the carbonyl oxygen is the common acceptor of two hydrogen bonds, whereas in conformer II, the enolic group acts as the C−H···O HB acceptor to $CHCl_3$. In the latter case, the C−H donor of $CHCl_3$ is positioned above the plane of the HCHD ring and binds almost perpendicularly to the enolic oxygen. It is notable that unlike conformer I, where the C−H donor binds laterally to the carbonyl oxygen, the shape of conformer II is different. As mentioned before, the former is a case of a bifurcated H-bond, leading to weakening of the intramolecular O−H···O HB, whereas in the latter, the same may be strengthened through a cooperative H-bonded linkage involving the weak C−H···O contact. Conformers I and II are predicted to be nearly iso-energetic at the B97*D*/6-311++G (d,p) and ωB97XD/6-311++G (d,p) levels of theory. However, for calculations using M06-2X method at the same level, conformer II is predicted to be more stable by ~1.3 kcal/mol (Table 1). A third conformer is also predicted at both levels of theory, where the carbonyl oxygen once again acts as the common HB acceptor, while one of the chlorine atoms on $CHCl_3$ binds to the enolic hydrogen, giving rise to a planar doubly H-bonded interface. Conformer III is predicted at all

DOI: 10.1021/acs.jpca.7b05615
J. Phys. Chem. A 2017, 121, 6012−6020

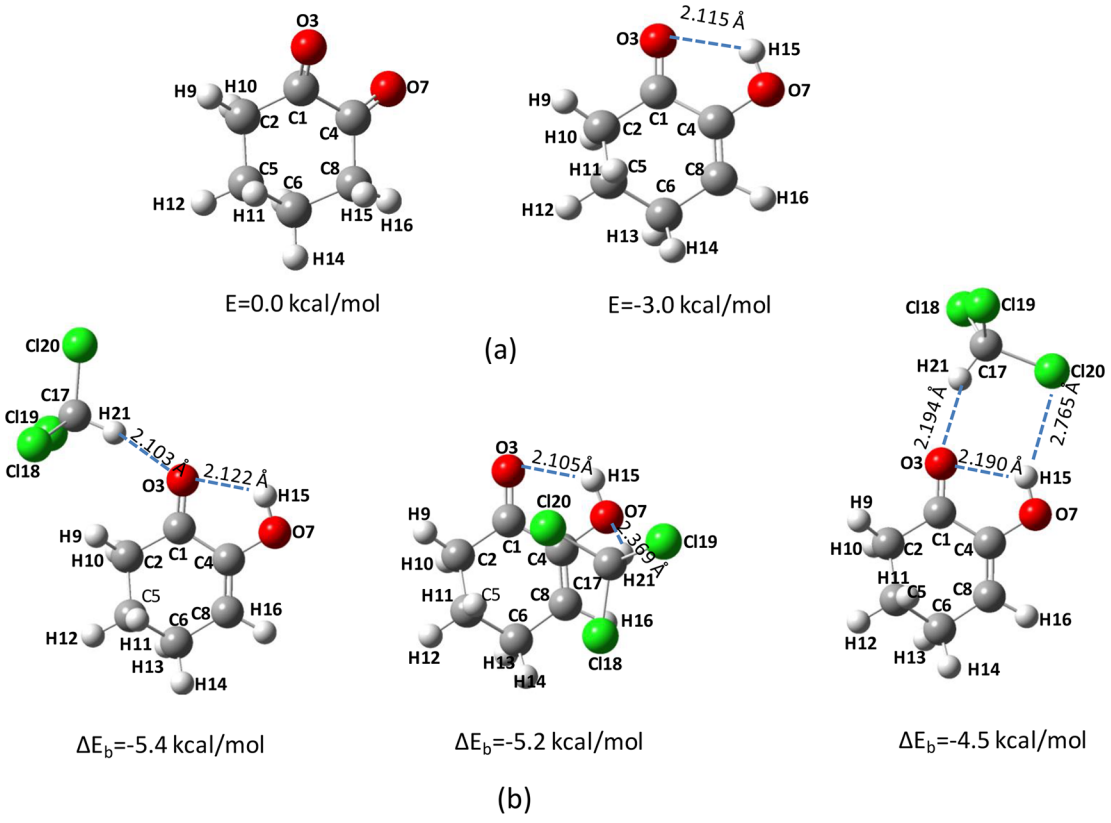

Figure 5. (a) Optimized structures and relative energies of the diketo and monoenol forms of 1,2-CHD and (b) optimized structures and stabilization energies of three conformers of HCHD-$CHCl_3$ complexes calculated at B97*D*/6-311++G(d.p) level of theory.

Table 1. Summary of Binding Energies (ΔE_b) and Predicted Spectral Shifts of the Probe ν_{O-H}, $\nu_{C=O}$, and ν_{C-H} Bands Corresponding to the Three Conformers of the HCHD-$CHCl_3$ Complex, Obtained at Various Levels of Theory[a]

			$\nu_{C=O}$ (cm^{-1})			ν_{OH} (cm^{-1})			ν_{C-H} (cm^{-1})		
		ΔE_b (kcal/mol)	monomer	complex	$\Delta\nu_{C=O}$ (cm^{-1}) [$\Delta\nu_{C=O}$ (obs)= −7,−7]	monomer	complex	$\Delta\nu_{O-H}$ (cm^{-1}) [$\Delta\nu_{O-H}$ (obs)= +23]	monomer	complex	$\Delta\nu_{C-H}$ (cm^{-1}) [$\Delta\nu_{C-H}$ (obs)= −33]
Con -I	B97D	5.4	1641.3, 1666.7	1628.6, 1655.0	−12.7, −11.7	3584.2	3598.0	+13.8	3100.2	3053.8	−46.4
	ωB97XD	6.0	1760.8, 1788.2	1753.2, 1769.1	−7.6, −19.1	3762.0	3767.3	+5.3	3204.1	3167.9	−36.2
	M06-2X	5.6	1763.2, 1807.8	1759.8, 1786.8	−3.4, −21.0	3781.2	3786.8	+5.6	3197.1	3231.5	+34.4
Con-II	B97D	5.2	1641.3, 1666.7	1644.8, 1670.0	+3.5, + 3.3	3584.2	3562.0	−22.2	3100.2	3115.9	+15.7
	ωB97XD	6.0	1760.8, 1788.2	1760.6, 1789.8	−0.2, + 1.6	3762.0	3740.1	−21.9	3204.1	3193.7	−10.4
	M06-2X	6.9	1763.2, 1807.8	1766.1, 1813.5	+2.9, + 5.7	3781.2	3745.3	−35.9	3197.1	3227.7	+30.6
Con-III	B97D	4.5	1641.3, 1666.7	1634.6, 1659.8	−6.7, −6.9	3584.2	3610.0	+25.8	3100.2	3131.6	+31.4
	ωB97XD	4.7	1760.8, 1788.2	1753.2, 1778.6	−7.6, −9.6	3762.0	3770.1	+8.1	3204.1	3219.8	+15.7
	M06-2X	4.8	1763.2, 1807.8	1757.1, 1792.6	−6.1, −15.2	3781.2	3769.1	−12.1	3197.1	3240.3	+43.2

[a]The observed shifts in argon matrix are denoted in parentheses in columns 6, 9, and 12.

levels of theory to be of somewhat higher energy compared to conformers I and II. Below, a comparison of experimental observations with the predictions of electronic structure theory is presented to determine which of the three conformers is actually formed within an argon matrix and also in CCl_4 solution.

Theoretically predicted spectroscopic shifts of ν_{O-H} and $\nu_{C=O}$ transitions of the HCHO moiety for the three probable conformers are presented in Table 1. At the B97*D*/6-311+ +G(d, p) level, ν_{O-H} blue shifts of 13.8 and 25.8 cm^{-1} are predicted for both conformers I and III, whereas a red shift of 22.2 cm^{-1} is predicted for conformer II. The predicted spectral shifts are similar for the two other levels of theory. However, as

DOI: 10.1021/acs.jpca.7b05615
J. Phys. Chem. A 2017, 121, 6012−6020

discussed in the previous section, we did not find any indication of red shifting for this vibrational transition in the infrared spectra measured both in CCl_4 solution and argon matrix. Furthermore, the same level of theory predicts red shifts of ∼12 and ∼7 cm^{-1} for the $\nu_{C=O}$ transitions of conformers I and III, which is also in accordance with our observation. On the other hand, a small blue shift is predicted for this band in the case of conformer II, which has not been observed in the measured spectra. Thus, although conformer II is nearly iso-energetic with conformer I, no experimental evidence in favor of the former was obtained. In the ν_{C-H} region, blue shifts of 15.7 and 31.4 cm^{-1} are predicted at the B97D level for conformers II and III, whereas a red shift of 46.4 cm^{-1} is predicted for conformer I, which agrees with the observed red shift of ∼33 cm^{-1}. A ν_{C-H} red shift of 10.4 cm^{-1} is predicted at the ωB97XD level for conformer II, but the lack of corresponding spectral signatures for the other two probe bands ν_{O-H} and $\nu_{C=O}$ in both media confirms the absence of this conformer. Also, a blue-shift of ν_{C-H} is predicted for conformer I only for the M06-2X method, but because no indication of ν_{C-H} blue shifting was observed, and calculations at the other two levels predict red shifts very close to the experimental value, we could infer at this point that under both experimental conditions, conformer I is formed exclusively.

The predicted changes in geometric parameters of the HCHD moiety of conformer I are also consistent with the spectral changes. At the B97*D*/6-311++G(d, p) level of theory, the O3···H21 intermolecular hydrogen bond distance of conformer I (2.103 Å) is predicted to be shorter compared to that of conformer III (2.194 Å), or the O7···H21 hydrogen bond distance (2.369 Å) of conformer II, implying that the donor−acceptor moieties approach each other more closely for the complexes in the former case compared to the latter two, leading to tighter binding at the H-bond site. Furthermore, the intramolecular O3···H15 hydrogen bond of HCHD moiety in conformers I and III is weakened, as observed from its lengthening from 2.115 Å in the monomer to 2.122 and 2.190 Å, respectively, upon complex formation. In contrast, the same for conformer II is decreased to 2.105 Å, and frequency calculation predicts red shifting of its O−H stretching fundamental, which has not been observed. Also, in conformers -I and III, a slight lengthening is also predicted for the C1═O3 bond along with a red-shifting of its stretching frequency, since the carbonyl group is the common acceptor of two hydrogen bonds. On the other hand, the same bond is predicted to be shortened by ∼0.001 Å for conformer II, accompanied by small blue shifts of its stretching transitions as discussed before. Furthermore, for conformer I, the C−H bond in $CHCl_3$ is lengthened from 1.089 to 1.092 Å, in accordance with the observed red shift of the ν_{C-H} band, whereas calculations predict shortening of the C−H bond in case of conformers II and III. The geometric predictions are similar for all other levels of theory.

D. Factors Contributing to Conformational Preferences. We have argued above that under both the physical conditions, experimental data suggest exclusive presence of conformer I. The important issue now is to find an explanation for origin of preferential stabilities of conformer I over conformers II and III. As pointed out previously according to gas phase calculations, the overall energy stabilization of conformer II is the same as that of conformer I, and higher than that of conformer III. But it should be emphasized that overall stability is contributed by electrostatic and dispersion interactions between all pairs of molecules on the two complexing moieties. In fact, the partitioning of the total binding energies of the three conformers carried out at the M06-2*X*/6-311++G(d,p) level using the LMO-EDA method (Table 2) shows that the dispersion component is much more

Table 2. Partitioning of the Total Intermolecular Interaction Energy into Its Various Components Obtained from Energy Decomposition Analysis at the M06-2*X*/6-311++G (d, p) Level for All Three Conformers of the HCHD-$CHCl_3$ Complex

energy (kcal/mol)	conformer I	conformer II	conformer III
electrostatic energy	−7.54	−7.66	−7.11
exchange-repulsion energy	+12.13	+18.24	+10.89
polarization energy	−2.26	−1.95	−2.56
dispersion energy	−7.96	−15.56	−6.20

enhanced for the nonplanar conformer II (∼15.5 kcal/mol) of the complex compared to the planar conformers-I and III (∼6−8 kcal/mol), which could primarily be responsible for the larger binding energy of the former species. However, despite the high magnitude of dispersion interaction in conformer II, its stabilizing contribution to overall binding energy is largely compensated by the destabilizing exchange-repulsion factor, which is highest for conformer II. At the M06-2*X*/6-311++G(d,p) level, the magnitude of this repulsive interaction is predicted to be +18.2 kcal/mol for conformer II, which is much higher than that for conformer I (+12.1 kcal/mol) or conformer III (+10.9 kcal/mol). In the presence of a surrounding medium like the argon matrix or a nonpolar solvent like CCl_4, dispersion interactions may become less relevant in guiding intermolecular orientations at the binding site of the complex compared to directional short-range interactions like exchange-repulsion.

Another important short-range local interaction parameter here is the hyperconjugative charge transfer between the filled lone pair orbital n(O) on the acceptor site of HCHD and the higher lying vacant σ*(C−H) orbital on the donor $CHCl_3$.[52] Its importance in determining conformational preferences and spectral shifts has recently been emphasized for both conventional and nonconventional HB variants.[6,7,9,47] NBO analysis at the B97*D*/6-311++G(d, p) level (Table 3) shows that the magnitude of this interaction is larger for conformers-I and III [n(O3)→ σ*(C17−H21) = 5.1 and 2.2 kcal/mol, respectively], where the carbonyl oxygen is the acceptor, than for conformer II where the enolic oxygen is the acceptor [n(O7)→ σ*(C17−H21) =1.4 kcal/mol]. The strength of the C−H···O intermolecular H-bond is therefore expected to be highest for conformer I. This difference is reflected also in C−H bond lengths in the optimized geometries of the conformers, as discussed previously. Of course, another competing factor is the effect of such intermolecular interaction on the O−H···O intramolecular H-bonding interaction in HCHD. In the case of conformer II, calculations suggest a slight increase (0.1 kcal/mol) in the hyperconjugative interaction between n(O3) and σ*(O7−H15) [n(O3)→ σ*(O7−H15)= 2.5 kcal/mol] from its monomer value (2.4 kcal/mol) because of cooperative enhancement of the O−H···O interaction by the weak C−H···O intermolecular interaction. The same energy parameter is somewhat lowered for conformers I and III (2.1 and 1.6 kcal/mol, respectively), because in these cases, the intermolecular H-bonding interaction becomes competitive with the intra-

DOI: 10.1021/acs.jpca.7b05615
J. Phys. Chem. A 2017, 121, 6012−6020

Table 3. Relevant Inter- and Intramolecular Hyperconjugation Energy Parameters Obtained from NBO Analysis on Geometries Optimized at Various Levels of Theory[a]

	complex I			complex II			complex III		
hyperconjugation energy (kcal/mol)	B97D	ωB97XD	M06-2X	B97D	ωB97XD	M06-2X	B97D	ωB97XD	M06-2X
n[O3(O7)]→ σ*(C17−H21)	5.1	6.3	3.0	1.4	2.1	1.4	2.2	3.7	2.9
n(O3)→ σ*(O7−H15)	2.1 (2.4)	3.3 (3.9)	2.3 (2.6)	2.5 (2.4)	4.1 (3.9)	2.7 (2.6)	1.6 (2.4)	2.8 (3.9)	2.1 (2.6)

[a]Values in parentheses denote corresponding energy parameters for the HCHD monomer.

molecular interaction. However, it is evident that the extent of weakening (0.3 kcal/mol) of this intramolecular hyperconjugative CT parameter for conformer I is much lesser than the stabilization due to the intermolecular n(O3)→ σ*(C17−H21) interaction (5.1 kcal/mol). Also, cooperative stabilization in conformer II involves a bent intramolecular O−H···O hydrogen bond, whereas the intermolecular C−H···O hydrogen bond is nearly linear in all predicted conformers, and it is therefore the strength of the latter that guides conformational preferences.

In the matrix isolation experiment, the orientational distributions of the two complexing molecules are likely to be random when the gaseous mixture is deposited initially on the cold KBr window. On annealing the matrix for a longer time period (15−30 min), chloroform and HCHD molecules diffuse toward each other to form the complex. However, as mentioned earlier, in a medium of Ar atoms, as well as CCl_4 solution, the dispersion component of total energy is likely to be very similar for all three possible orientations of $CHCl_3$ about HCHD, and conformational selectivity is guided solely by the short-range hyperconjugative interactions and exchange-repulsion factors.

E. Effect of Complex Formation on $\nu_{C=O}$ Intensity. It has been pointed out in Section 3.1 that the two $\nu_{C=O}$ components of HCHF are affected differently upon complex formation. The intensity of the higher frequency band $\nu_{C=O}{}^{A}$ is lowered while that of the lower frequency component $\nu_{C=O}{}^{B}$ band increases (Figure 1). Interestingly, the same is also predicted by the electronic structure calculations. To understand the origin of these effects, we have performed potential energy distributions of the normal modes corresponding to the two $\nu_{C=O}$ fundamentals of both the monomer and complex at the B97D/6-311++G(d, p) level. It is seen that complexation causes a significant change in potential energy distribution of the two modes.

In case of the monomer, the potential energy distribution corresponding to the component A corresponds to 61% C═O stretching and 27% C═C stretching, whereas for component B the contributions of the two local vibrations are 27% and 36%, respectively (Table 4). Obviously, the former appears more intense in the IR spectrum because of higher contribution of C═O stretching local mode, and the calculated relative intensity for infrared fundamentals of the two modes is ∼2:1. In the case of the complex (conformer I), the contributions of the two local vibrations in the higher frequency component change to 36 and 42%, respectively. On the other hand, in the lower frequency component, the contribution of C═O stretching is increased to 44% from 27%. Clearly, complex formation causes a significant reversal of the contribution of C═O stretching in the two normal modes of the molecule, and the relative intensity calculated for the two IR active fundamentals of the complex is altered. Thus, the observation is a clear manifestation of the important attribute of intensity changes upon hydrogen bonding, in addition to the obvious effect of electronic charge reorganization.

Table 4. Integrated IR Intensities and Potential Energy Distributions (PEDs) of Selected Vibrational Modes of HCHD and Their Changes upon Formation of 1:1 Complex with Chloroform, Predicted by Calculation at B97D/6-311++G(d,p) Level

molecular Species	frequency (cm^{-1})	integrated IR Intensity (km/mol)	mode description (PEDs)
monomer	1665.5($\nu_{C=O}{}^{A}$)	211.3	ν_{C1-O3} (61.3), ν_{C4-C8} (27.1)
	1639.8 ($\nu_{C=O}{}^{B}$)	100.0	ν_{C4-C8} (36.2), ν_{C1-O3} (27.7)
conformer I of complex	1655.0 ($\nu_{C=O}{}^{A}$)	129.0	ν_{C4-C8} (42), ν_{C1-O3} (36)
	1628.6 ($\nu_{C=O}{}^{B}$)	262.5	ν_{C1-O3} (44), ν_{C4-C8} (27)

4. CONCLUSION

A CH···O hydrogen-bonded complex between chloroform and monoenol tautomeric form of 1,2-cyclohexanedione has been investigated using infrared spectroscopy and quantum chemistry methods. The complex was studied both in an argon matrix at 8 K, and also in CCl_4 solution at room temperature (25 °C). Calculations at different levels of theory predict three CH···O hydrogen bonded conformers of the complex. In conformers I and III, the C−H bond of chloroform (HB donor) binds to the carbonyl oxygen of the acceptor (HCHD), whereas in conformer II the binding is at the enolic site. Infrared spectra reveal that because of complex formation, the $\nu_{C=O}$ band of acceptor undergoes an ∼7 cm^{-1} red shift in argon matrix, while the ν_{O-H} band undergoes an ∼23 cm^{-1} blue shift. Similar shifts are also observed in CCl_4 solution. The $\nu_{C=O}$ transition of both the bare HCHD and the HCHD-chloroform complex appears as doublet due to symmetric and antisymmetric coupling of adjacent C═O and C═C bonds in the enol tautomer. Complex formation with chloroform causes a significant change in the intensity ratios of the two components, which is attributed to alteration of the potential energy distribution of the local vibrations in the complex. A red shift of ∼33 cm^{-1} is also observed in the argon matrix for the ν_{C-H} transition of the donor $CHCl_3$. The observations match closely with the predicted shifts of the three probe transitions of conformer I of the complex, where the carbonyl group is the common acceptor of both the intramolecular O−H···O and intermolecular CH···O hydrogen bonds. No experimental evidence is obtained in favor of the higher energy conformer III, or even conformer II, which is iso-energetic with conformer I, although in conformer II the O−H···O hydrogen bond is predicted to be cooperatively enhanced by the intermolecular CH···O linkage, and the dispersion stabilization is highest among all three conformers. The exclusive preference of conformer I under both the physical conditions is attributed to

DOI: 10.1021/acs.jpca.7b05615
J. Phys. Chem. A 2017, 121, 6012−6020

stronger hyperconjugative charge transfer effects at the site of the intermolecular CH···O hydrogen bonding. The observation therefore underlines the precedence of local stabilizing factors over longer range dispersion and other interaction energies in guiding conformational preferences of weak CH···O H-bonded complexes, particularly in condensed media like argon matrix and CCl_4 solution.

■ ASSOCIATED CONTENT

Supporting Information

The Supporting Information is available free of charge on the ACS Publications website at DOI: 10.1021/acs.jpca.7b05615.

Comparison of the matrix isolation IR spectrum in the ν_{C-H} region with predicted transitions corresponding mostly to different overtones and combinations that gain intensity on complex formation (PDF)

■ AUTHOR INFORMATION

Corresponding Author

*E-mail: pctc@iacs.res.in.

ORCID

Biman Bandyopadhyay: 0000-0002-4320-6231

Tapas Chakraborty: 0000-0002-5292-3873

Notes

The authors declare no competing financial interest.

■ ACKNOWLEDGMENTS

The authors acknowledge the financial support received from the Department of Science and Technology, Government of India, and the Council of Scientific and Industrial Research, Government of India, to carry out the research.

■ REFERENCES

(1) Buckingham, A. D.; Del Bene, J. E.; McDowell, S. A. C. The Hydrogen Bond. *Chem. Phys. Lett.* **2008**, *463*, 1−10 and references therein..

(2) Desiraju, G. R.; Steiner, T. *The Weak Hydrogen Bond*; Oxford University Press: Oxford, U.K., 1999.

(3) Scheiner, S. *Hydrogen Bonding*; Oxford University Press: New York, 1997.

(4) Banerjee, P.; Bhattacharya, I.; Chakraborty, T. Cooperative Effect on Phenolic ν_{O-H} Frequencies in 1:1 Hydrogen Bonded Complexes of o-Fluorophenols with Water: A Matrix-Isolation Infrared Spectroscopy Study. *Spectrochim. Acta, Part A* **2017**, *181*, 116−121.

(5) Saini, J.; Viswanathan, K. S. Discerning Near-Isoergic Isomers. A Matrix Isolation Infrared and *ab Initio* Study of the Propargyl Alcohol Dimers. *J. Phys. Chem. A* **2017**, *121*, 1448−1459.

(6) Banerjee, P.; Bhattacharya, I.; Chakraborty, T. Matrix Isolation Infrared Spectroscopy of an OH···π Hydrogen Bonded Complex between Formic acid and Benzene. *J. Phys. Chem. A* **2016**, *120*, 3731−3739.

(7) Banerjee, P.; Bhattacharya, I.; Chakraborty, T. Matrix Isolation Infrared Spectra of O-H···π Hydrogen Bonded Complexes of Acetic acid and Trifluoroacetic acid with Benzene. *J. Chem. Sci.* **2016**, *128*, 1549−1555.

(8) Rutkowski, K. S.; Melikova, S. M.; Linok, O. V.; Czarnik-Matusewicz, B.; Rospenk, M. Infrared Spectroscopy and Ab Initio Study of Hydrogen Bonded Cl_3CD-$N(CH3)_3$ Complex in the Gas Phase. *Spectrochim. Acta, Part A* **2015**, *136*, 95−99.

(9) Banerjee, P.; Chakraborty, T. Correlation of ν_{OH} Spectral Shifts of Phenol−Benzene O−H···π Hydrogen-Bonded Complexes with Donor's Acidity: A Combined Matrix Isolation, Infrared Spectroscopy, and Quantum Chemistry Study. *J. Phys. Chem. A* **2014**, *118*, 7074−7084.

(10) Rutkowski, K. S.; Melikova, S. M.; Janski, J.; Koll, A. Cryospectroscopic and Ab Initio Anharmonic Studies of Acetylene−Trimethylamine H-bonded Complex. *Chem. Phys.* **2010**, *375*, 92−100.

(11) Chervenkov, S.; Karaminkov, R.; Braun, J.; Neusser, H. J.; Panja, S. S.; Chakraborty, T. Specific and Non-specific Interactions in a Molecule with Flexible Side Chain: 2-Phenylethanol and its 1:1 Complex with Argon Studied by High-resolution UV Spectroscopy. *J. Chem. Phys.* **2006**, *124*, 234302.

(12) Panja, S. S.; Chakraborty, T. Discrimination of Rotational Isomers of 2-Phenylethanol by Dispersed Fluorescence Spectroscopy in Supersonic Jet. *J. Phys. Chem. A* **2003**, *107*, 10984−10987.

(13) Das, A.; Mahato, K. K.; Panja, S. S.; Chakraborty, T. Conformations of Indan and 2-Indanol: A Combined Study by UV Laser Spectroscopy and Quantum Chemistry Calculation. *J. Chem. Phys.* **2003**, *119*, 2523−2530.

(14) Caminati, W.; Melandri, S.; Moreschini, P.; Favero, P. G. The C-F···H-C Anti-Hydrogen Bond in the Gas Phase: Microwave Structure of the Difluoromethane Dimer. *Angew. Chem., Int. Ed.* **1999**, *38*, 2924−2925.

(15) Gu, Y.; Kar, T.; Scheiner, S. J. Fundamental Properties of the CH···O Interaction: Is it a True Hydrogen Bond? *J. Am. Chem. Soc.* **1999**, *121*, 9411−9422.

(16) Hobza, P.; Havlas, Z. Blue-Shifting Hydrogen Bonds. *Chem. Rev.* **2000**, *100*, 4253−4264.

(17) Scheiner, S.; Kar, T. Red- versus Blue-Shifting Hydrogen Bonds: Are There Fundamental Distinctions? *J. Phys. Chem. A* **2002**, *106*, 1784−1789.

(18) Cubero, E.; Orozco, M.; Hobza, P.; Luque, F. J. Hydrogen Bond versus Anti-Hydrogen Bond: A Comparative Analysis Based on the Electron Density Topology. *J. Phys. Chem. A* **1999**, *103*, 6394−6401.

(19) Alabugin, I. V.; Manoharan, M.; Peabody, S.; Weinhold, F. Electronic Basis of Improper Hydrogen Bonding: A Subtle Balance of Hyperconjugation and Rehybridization. *J. Am. Chem. Soc.* **2003**, *125*, 5973−5987.

(20) Joseph, J.; Jemmis, E. D. Red-, Blue-, or No-Shift in Hydrogen Bonds: A Unified Explanation. *J. Am. Chem. Soc.* **2007**, *129*, 4620−4632 and references therein..

(21) Scheiner, S.; Grabowski, S. J.; Kar, T. Influence of Hybridization and Substitution on the Properties of the CH···O Hydrogen Bond. *J. Phys. Chem. A* **2001**, *105*, 10607−10612.

(22) Li, A. Y. Chemical Origin of Blue- and Red-Shifted Hydrogen Bonds: Intramolecular Hyperconjugation and its Coupling with Intermolecular Hyperconjugation. *J. Chem. Phys.* **2007**, *126*, 154102.

(23) Sutor, D. J. The C−H··· O Hydrogen Bond in Crystals. *Nature* **1962**, *195*, 68−69.

(24) Steiner, T.; Lutz, B.; van der Maas, J.; Veldman, N.; Schreurs, A. M. M.; Kroon, J.; Kanters, J. A. Spectroscopic Evidence for Cooperativity Effects Involving C−H···O Hydrogen Bonds: Crystalline Mestranol. *Chem. Commun.* **1997**, 191−192.

(25) Jiang, L.; Lai, L. CH···O Hydrogen Bonds at Protein-Protein Interfaces. *J. Biol. Chem.* **2002**, *277*, 37732−37740.

(26) Brandl, M.; Meyer, M.; Sühnel, J. Quantum-Chemical Analysis of C-H···O and C-H···N Interactions in RNA Base Pairs-H-Bond Versus Anti-H-Bond Pattern. *J. Biomol. Struct. Dyn.* **2001**, *18*, 545−555.

(27) Ornstein, R. L.; Zheng, Y. J. Ab Initio Quantum Mechanics Analysis of Imidazole C-H···O Water Hydrogen Bonding and a Molecular Mechanics Forcefield Correction. *J. Biomol. Struct. Dyn.* **1997**, *14*, 657−665.

(28) Senes, A.; Ubarretxena-Belandia, I.; Engelman, D. M. The C_{alpha}—H···O Hydrogen Bond: A Determinant of Stability and Specificity in Transmembrane Helix Interactions. *Proc. Natl. Acad. Sci. U. S. A.* **2001**, *98*, 9056−9061.

(29) Driver, R. W.; Claridge, T. D. W.; Scheiner, S.; Smith, M. D. Torsional and Electronic Factors Control the C-H···O Interaction. *Chem. - Eur. J.* **2016**, *22*, 16513−16521.

(30) Karir, G.; Fatima, M.; Viswanathan, K. S. The Elusive ≡C-H··· O Complex in the Hydrogen Bonded Systems of Phenylacetylene: A

DOI: 10.1021/acs.jpca.7b05615
J. Phys. Chem. A 2017, 121, 6012−6020

Matrix Isolation Infrared and Ab Initio Study. *J. Chem. Sci.* **2016**, *128*, 1557−1569.
(31) Melikova, S. M.; Rutkowski, K. S. Investigation of the IR Spectra of Weakly Hydrogen-Bonded Complex, $Cl_3CH\cdots O(CD_3)_2$ in a Cryosolution in Liquid Krypton. *Opt. Spectrosc.* **2016**, *120*, 242−249.
(32) Bandyopadhyay, B.; Pandey, P.; Banerjee, P.; Samanta, A. K.; Chakraborty, T. CH···O Interaction Lowers Hydrogen Transfer Barrier to Keto−Enol Tautomerization of β-Cyclohexanedione: Combined Infrared Spectroscopic and Electronic Structure Calculation Study. *J. Phys. Chem. A* **2012**, *116*, 3836−3845.
(33) Jones, C. R.; Baruah, P. K.; Thompson, A. L.; Scheiner, S.; Smith, M. D. Can a C−H···O Interaction Be a Determinant of Conformation? *J. Am. Chem. Soc.* **2012**, *134*, 12064−1207.
(34) Ito, F. Matrix-isolation Infrared Studies of 1:1 Molecular Complexes Containing Chloroform ($CHCl_3$) and Lewis Bases: Seamless Transition from Blue-shifted to Red-shifted Hydrogen Bonds. *J. Chem. Phys.* **2012**, *137*, 014505.
(35) Samanta, A. K.; Pandey, P.; Bandyopadhyay, B.; Chakraborty, T. Cooperative Strengthening of An Intramolecular O−H—O Hydrogen Bond by a Weak C−H—O Counterpart: Matrix Isolation Infrared Spectroscopy and Quantum Chemical Studies on 3-methyl-1,2-cyclohexanedione. *J. Phys. Chem. A* **2010**, *114*, 1650−1656.
(36) Ito, F. Infrared Spectroscopy of $(CHF_2Cl)_2$ and CHF_2Cl-H2O Complex in Xe Matrix. *Chem. Phys.* **2010**, *369*, 82−90.
(37) Mukhopadhyay, A.; Pandey, P.; Chakraborty, T. Blue- and Red-Shifting CH···O Hydrogen Bonded Complexes between Haloforms and Ethers: Correlation of Donor nu(C-H) Spectral Shifts with C-O-C Angular Strain of the Acceptors. *J. Phys. Chem. A* **2010**, *114*, 5026−5033.
(38) Mukhopadhyay, A.; Mukherjee, M.; Pandey, P.; Samanta, A. K.; Bandyopadhyay, B.; Chakraborty, T. Blue Shifting C−H···O Hydrogen-Bonded Complexes Between Chloroform and Small Cyclic Ketones: Ring-Size Effects on Stability and Spectral Shifts. *J. Phys. Chem. A* **2009**, *113*, 3078−3987.
(39) Vaz, P. D.; Ribeiro-Claro, P. J. A. Strong Experimental Evidence of C-H···O Hydrogen Bonds in Cyclopentanone: The Splitting of the ν(C═O) Mode Revisited. *J. Phys. Chem. A* **2003**, *107*, 6301−6305.
(40) Delanoye, S. N.; Herrebout, W. A.; van der Veken, B. J. Improper or Classical Hydrogen Bonding? A Comparative Cryosolutions Infrared Study of the Complexes of $HCClF_2$, $HCCl_2F$, and $HCCl_3$ with Dimethyl Ether. *J. Am. Chem. Soc.* **2002**, *124*, 7490−7498.
(41) Delanoye, S. N.; Herrebout, W. A.; van der Veken, B. J. Blue Shifting Hydrogen Bonding in the Complexes of Chlorofluoro Haloforms with Acetone-d_6 and Oxirane-d_4. *J. Am. Chem. Soc.* **2002**, *124*, 11854−11855.
(42) Marques, M. P. M.; Amorim da Costa, A. M.; Ribeiro-Claro, P. J. A. Evidence of C−H···O Hydrogen Bonds in Liquid 4-Ethoxybenzaldehyde by NMR and Vibrational Spectroscopies. *J. Phys. Chem. A* **2001**, *105*, 5292−5297.
(43) Karger, N.; Amorim da Costa, A. M.; Ribeiro-Claro, P. J. A. C−H···O Bonded Dimers in Liquid 4-Methoxybenzaldehyde: A Study by NMR, Vibrational Spectroscopy, and ab Initio Calculations. *J. Phys. Chem. A* **1999**, *103*, 8672−8677.
(44) Mizuno, K.; Ochi, T.; Shindo, Y. Hydrophobic Hydration of Acetone Probed by Nuclear Magnetic Resonance and Infrared: Evidence for the Interaction C−H···OH_2. *J. Chem. Phys.* **1998**, *109*, 9502−9507.
(45) Gianturco, M. A.; Giammarino, A. S.; Pitcher, R. G. The Structures of Five Cyclic Diketones Isolated from Coffee. *Tetrahedron* **1963**, *19*, 2051−2059.
(46) Samanta, A. K.; Pandey, P.; Bandyopadhyay, B.; Chakraborty, T. Keto−enoltautomers of 1,2-Cyclohexanedione in Solid, Liquid, Vapour and a Cold Inert Gas Matrix: Infrared Spectroscopy and Quantum Chemistry Calculation. *J. Mol. Struct.* **2010**, *963*, 234−239.
(47) Banerjee, P.; Mukhopadhyay, D. P.; Chakraborty, T. On the Origin of Donor O−H bond Weakening in Phenol-Water Complexes. *J. Chem. Phys.* **2015**, *143*, 204306.
(48) Frisch, M. J.; Trucks, G. W.; Schlegel, H. B.; Scuseria, G. E.; Robb, M. A.; Cheeseman, J. R.; Scalmani, G.; Barone, V.; Mennucci, B.; Petersson, G. A.; et al. *Gaussian 09, Revision D.01*; Gaussian, Inc.: Wallingford, CT, 2013.
(49) Grimme, S. Density Functional Theory with London Dispersion Corrections. *WIREs Comput. Mol. Sci.* **2011**, *1*, 211−228.
(50) Zhao, Y.; Truhlar, D. G. The M06 Suite of Density Functionals for Main Group Thermochemistry, Thermochemical Kinetics, Noncovalent Interactions, Excited States, and Transition Elements: Two New Functionals and Systematic Testing of Four M06-class Functionals and 12 Other Functionals. *Theor. Chem. Acc.* **2008**, *120*, 215−241.
(51) Boys, S. F.; Bernardi, F. The Calculation of Small Molecular Interactions by the Differences of Separate Total Energies: Some Procedures with Reduced Errors. *Mol. Phys.* **1970**, *19*, 553−566.
(52) Reed, A. E.; Curtiss, L. A.; Weinhold, F. Intermolecular Interactions from a Natural Bond Orbital, Donor-Acceptor Viewpoint. *Chem. Rev.* **1988**, *88*, 899−926.
(53) Pulay, P.; Torok, F. Parameter Form of Matrix F. II. Assignment with the Aid of the Parameter Form. *Acta Chim. Acad. Sci. Hung.* **1966**, *47*, 273.
(54) Schmidt, M. W.; Baldridge, K. K.; Boatz, J. A.; Elbert, S. T.; Gordon, M. S.; Jensen, J. H.; Koseki, S.; Matsunaga, N.; Nguyen, K. A.; Su, S. J.; et al. General Atomic and Molecular Electronic Structure System. *J. Comput. Chem.* **1993**, *14*, 1347−1363.
(55) Su, P.; Li, H. Energy Decomposition Analysis of Covalent Bonds and Intermolecular Interactions. *J. Chem. Phys.* **2009**, *131*, 014102.
(56) Rutkowski, K. S.; Melikova, S. M.; Rospenk, M.; Koll, A. Strong and Weak Effects Caused by Non Covalent Interactions between Chloroform and Selected Electron Donor Molecules. *Phys. Chem. Chem. Phys.* **2011**, *13*, 14223−14234.

DOI: 10.1021/acs.jpca.7b05615
J. Phys. Chem. A 2017, 121, 6012−6020